

FTII-Bench: A Comprehensive Multimodal Benchmark for Flow Text with Image Insertion

Jiacheng Ruan^{1*}, Yebin Yang^{1*}, Zehao Lin², Yuchen Feng², Feiyu Xiong², Zeyun Tang², Zhiyu Li^{2†}

¹ Shanghai Jiao Tong University

² Institute for Advanced Algorithms Research, Shanghai.
jackchenruan@sjtu.edu.cn, lizy@iaar.ac.cn

Abstract

Benefiting from the revolutionary advances in large language models (LLMs) and foundational vision models, large vision-language models (LVLMs) have also made significant progress. However, current benchmarks focus on tasks that evaluating only a single aspect of LVLM capabilities (e.g., recognition, detection, understanding). These tasks fail to fully demonstrate LVLMs' potential in complex application scenarios. To comprehensively assess the performance of existing LVLMs, we propose a more challenging task called the Flow Text with Image Insertion task (FTII). This task requires LVLMs to simultaneously possess outstanding abilities in image comprehension, instruction understanding, and long-text interpretation. Specifically, given several text paragraphs accumulate, the LVLMs are required to select the most suitable image from the candidates to insert after the corresponding paragraph. Constructing a benchmark for such a task is highly challenging, particularly in determining the sequence of flowing text and images. To address this challenge, we turn to professional news reports, which naturally contain a gold standard for image-text sequences. Based on this, we introduce the Flow Text with Image Insertion Benchmark (FTII-Bench), which includes 318 high-quality Chinese image-text news articles and 307 high-quality English image-text news articles, covering 10 different news domains. Using these 625 high-quality articles, we construct problems of two different types with multiple levels of difficulty. Furthermore, we establish two different evaluation pipelines based on the CLIP model and existing LVLMs. We evaluate 9 open-source and 2 closed-source LVLMs as well as 2 CLIP-based models. Results indicate that even the most advanced models (e.g., GPT-4o) face significant challenges when tackling the FTII task. The code and data will be available at <https://github.com/IAAR-Shanghai/FTIIBench>.

Introduction

In recent years, significant advancements in large visual-language models (LVLMs) (Alayrac et al. 2022; Liu et al. 2024b; Zheng et al. 2024; Dai et al. 2023) have been achieved, driven by the revolutionary progress of large language models (LLMs) (OpenAI 2023; Anil et al. 2023; Touvron et al. 2023; Zhu et al. 2024) and improvements in foundational visual models (Dosovitskiy et al. 2020; Gan et al.

*These authors contributed equally.

†Corresponding author.



Text Paragraph: The filming crew of the movie *The Sun Also Rises* unexpectedly encountered heavy snow, causing delays in the schedule. Jiang Wen asked for Lee Pingbin's opinion, and Lee Pingbin felt that experiencing snow in the desert was a rare opportunity. He suggested continuing to shoot and taking advantage of the unique weather conditions. It turned out that Lee Pingbin's judgment was spot on, as the snow scenes greatly enhanced the film's texture and quality.

Question:

Which image is suitable for insertion after the given text?



The most suitable image is C.



The most suitable image is A.



Figure 1: An example of a single-choice question in our FTII-Bench.

2022). These models have shown outstanding capabilities in tasks such as image understanding, vision-language reasoning, and visual recognition, leading to widespread applications across various industries (Singhal et al. 2023; Wang et al. 2023b; Ruan et al. 2024b). For instance, in the medical field, LVLMs are employed for automated pathological image analysis and diagnostic assistance (Singhal et al. 2023; Li et al. 2024), while in autonomous driving, they are utilized for environmental perception and scene understanding (Xu et al. 2024; Wang et al. 2023b).

With the increasing development of LVLMs, comprehensive evaluation of these models has become a research focus. However, existing benchmarks primarily focus on tasks such as object recognition, localization, and visual-text reasoning, usually evaluating only a single aspect of LVLMs' capabilities, such as recognition (Liu et al. 2023b), detection (Fu et al. 2024), or understanding (Yang et al. 2021), without simultaneously assessing their comprehensive abilities across multiple aspects. In real-world applications, LVLMs must handle more dynamic multimodal information. To thoroughly assess the performance of exist-

ing LVLMs, we propose a more challenging task, called the Flow Text with Image Insertion Task (FTII). This task comprises multiple text paragraphs and a set of candidate images. The text is provided cumulatively, requiring LVLMs to select the most suitable image from the candidates to insert after the corresponding paragraph. This presents three simultaneous challenges for current LVLMs: firstly, the ability to comprehend images, requiring the model to fully understand the meaning of all images in the set; secondly, the ability to understand long texts, as the cumulative nature of the text continuously increases the input length; and finally, the ability to follow instructions, demanding that LVLMs output the confidence level for the selected image in the specified format.

Constructing such a benchmark presents significant challenges, particularly in determining the sequence of streaming text and illustrations. However, we found that data from the news domain offers an ideal gold standard. On some multimedia platforms, such as Twitter, the order of text and images often lacks professionalism, making them unsuitable as a reliable benchmark. In contrast, news reports, especially official ones, inherently contain authoritative and high-quality sequencing of text and images. To this end, we manually collected 318 high-quality Chinese and 307 high-quality English image-text reports from Xinhua News and BBC News, covering ten different news domains such as politics, economics, and technology. Based on these 625 reports, we developed FTII-Bench, which includes both single-choice and flow-insertion question types. The single-choice questions are divided into four difficulty levels, while the flow-insertion questions have three difficulty levels. This design allows for a more comprehensive evaluation of LVLMs at different levels.

To ensure the comprehensiveness of our validation results, we not only established an evaluation pipeline for LVLMs but also introduced an evaluation pipeline based on the CLIP (Radford et al. 2021) paradigm. Using these pipelines, we conducted extensive validation of 9 open-source LVLMs (Liu et al. 2024c; Dai et al. 2023; Yao et al. 2024; Bai et al. 2023; Zhang et al. 2024; Peng et al. 2023; Laurençon et al. 2024; Bavishi et al. 2023), 2 closed-source LVLMs, and 2 CLIP-based models (Chen et al. 2024; Xiao et al. 2023) on FTII-Bench. The results indicate that even the most advanced models face significant challenges when handling FTII tasks. For instance, GPT-4o achieved only 61.0% accuracy on the most difficult single-choice questions (one out of three options). This suggests that current LVLMs still have substantial room for improvement in tackling complex multimodal tasks and that there is a need to further unleash their potential when tested on multiple capabilities simultaneously.

In summary, the main contributions of this paper are as follows: **1)** For the first time, We propose a novel and challenging task, dubbed the Flow Text with Image Insertion, which requires LVLMs to have the ability to understand long texts, comprehend images, and follow complex instructions. **2)** We manually collected 625 high-quality news image-text reports and constructed the FTII-Bench, which contains 10,231 questions, providing a rich evaluation resource for

future researchers. **3)** We evaluated 9 open-source LVLMs, 2 advanced closed-source LVLMs, and 2 CLIP-based models, revealing the performance bottlenecks of these models in the FTII task and providing directions for future model improvements.

Related Works

Large Vision and Language Models

In recent years, large vision language models (LVLMs) have achieved remarkable progress in multimodal tasks by effectively integrating visual and textual information. Llava (Liu et al. 2024c), leveraging large-scale image-text datasets for training, excels in image captioning and visual question answering tasks. Qwen-VL (Bai et al. 2023) extracts and compresses visual features through a set of trainable queries and introduces a single-layer cross-attention module to achieve visual-text modality alignment, supporting interleaved image-text input. CogVLM (Wang et al. 2023a) integrates images and text by concatenating them in the input embedding space and incorporates trainable visual layers within the language model to achieve the alignment between the two modalities. MiniCPM-V (Yao et al. 2024) enhances the efficiency of multimodal models through effective visual token compression and modality alignment, achieving a balance between performance and computational cost. It is already supported for deployment on various edge devices.

Although LVLMs have rapidly evolved, a comprehensive and multi-dimensional evaluation of these models’ capabilities remains underexplored. Currently, many benchmarks involve image-text matching and cross-modal reasoning tasks, but they are either constrained by single image or limited context length (Mathew, Karatzas, and Jawahar 2021; Liu et al. 2023a), thereby inadequately assessing the models’ ability to understand long textual and multi-image contexts, or they focus solely on evaluating individual visual capabilities, such as recognition (Liu et al. 2023b), OCR (Masry et al. 2022), math (Lu et al. 2023), detection (Fu et al. 2024), or understanding (Yang et al. 2021). These evaluation approaches are insufficient to fully reflect the models’ performance in complex tasks and real-world applications. Therefore, we propose FTII-Bench, which simultaneously evaluates models across multiple dimensions, including multi-image visual understanding, long-context comprehension, and complex instruction following.

CLIP-based Models

CLIP-based models have demonstrated remarkable capabilities in visual and language understanding in recent years. CLIP (Radford et al. 2021) utilizes contrastive learning on a large-scale dataset of image-text pairs, significantly enhancing the accuracy of matching between images and text while supporting zero-shot learning. This ability makes CLIP excel in tasks such as image-text retrieval and image classification, establishing it as an important foundational model for image-text understanding tasks.

To further improve the performance of multimodal models, ALIGN (Jia et al. 2021) model employs a similar contrastive learning strategy and leverages a larger dataset to

optimize image-text representation learning. Florence (Yuan et al. 2021) incorporates improved visual and language alignment techniques, optimizing the model’s performance in visual understanding and text description tasks.

Building on CLIP, many studies have further explored its applications and optimizations for specific tasks (Zhou et al. 2022; Khattak et al. 2023; Ruan et al. 2023; Gao et al. 2024; Ruan et al. 2024a). For example, ViFi-CLIP (Rasheed et al. 2023) enhances performance in video action recognition tasks by fine-tuning the CLIP. Additionally, BGE (Chen et al. 2024; Xiao et al. 2023) introduces a novel embedding model M3-Embedding, which excels in multilinguality, multifunctionality, and multi-granularity. It’s capable of dense retrieval, multi-vector retrieval, and sparse retrieval, providing a unified model foundation for real-world IR applications.

Datasets

In this section, we provide a detailed introduction to FTII-Bench. First, we define the Flow Text with Image Insertion Task. Next, we describe the data collection process and present relevant statistical information. Finally, we explain the two types of questions in the benchmark: single-choice questions and flow-insertion questions, and discuss the various difficulty settings.

Task Definition

Given a source \mathbf{S} that interleaves text and images, consisting of n text paragraphs and m images, i.e., $\mathbf{S} = \{s_1^t, \dots, s_n^t; s_1^i, \dots, s_m^i\}$. \mathbf{S} follows a true image insertion order, denoted as \mathbf{O}_{gt} . By separating the ground truth images from the text, we can obtain the image set $\mathbf{I}_s = \{s_1^i, \dots, s_m^i\}$ and the text paragraphs set $\mathbf{T} = \{s_1^t, \dots, s_n^t\}$. At this point, a set of p distractor images I_d is introduced, i.e., $\mathbf{I}_d = \{d_1^i, \dots, d_p^i\}$. Subsequently, by merging the ground truth image set and the distractor image set, we obtain the candidate image set $\mathbf{I}_c = \{s_1^i, \dots, s_m^i, d_1^i, \dots, d_p^i\}$. Finally, the text paragraphs set is incrementally accumulated as text input to the LVLMS, while the candidate image set is provided iteratively as image input. The LVLMS then provide confidence scores to determine the image insertion positions, ultimately resulting in the predicted image insertion order \mathbf{O}_p . The task workflow is illustrated in Algorithm 1.

When calculating evaluation metrics, we consider three scenarios: accuracy when only inserted images are considered (Acc_i), accuracy when only non-inserted images are considered (Acc_{ni}), and accuracy when both are considered (Acc_b). For clarity, we present the following example: Given a source with 2 images and 5 text paragraphs, i.e., $\mathbf{S} = \{s_1^t, s_2^t, s_1^i, s_3^t, s_4^t, s_5^t, s_2^i\}$, the image insertion order follows $\mathbf{O}_{\text{gt}} = \{\text{None}, \text{None}, s_1^i, \text{None}, \text{None}, s_2^i\}$. By separating images and text, we obtain the groundtruth image set $\mathbf{I}_s = \{s_1^i, s_2^i\}$ and the text paragraph set $\mathbf{T} = \{s_1^t, s_2^t, s_3^t, s_4^t, s_5^t\}$. At this point, a distractor image set \mathbf{I}_d is introduced, assuming \mathbf{I}_d contains 5 distractor images, i.e., $\mathbf{I}_d = \{d_1^i, d_2^i, d_3^i, d_4^i, d_5^i\}$. The groundtruth image set is then merged with the distractor image set to form the candidate image set $\mathbf{I}_c = \{s_1^i, s_2^i, d_1^i, d_2^i, d_3^i, d_4^i, d_5^i\}$. Finally, following the steps in Algorithm 1, we obtain the

Algorithm 1: Flow Text with Image Insertion Task

Require: Text paragraphs $\mathbf{T} = \{s_1^t, \dots, s_n^t\}$, ground truth images $\mathbf{I}_s = \{s_1^i, \dots, s_m^i\}$, distracting images $\mathbf{I}_d = \{d_1^i, \dots, d_p^i\}$, and a LVLMS.

Ensure: Predicted image-text order \mathbf{O}_p .

- 1: Initialize candidate image set $\mathbf{I}_c = \mathbf{I}_s \cup \mathbf{I}_d = \{s_1^i, \dots, s_m^i, d_1^i, \dots, d_p^i\}$.
- 2: Initialize empty order $\mathbf{O}_p \leftarrow \{\}$.
- 3: Initialize accumulated text input $\mathbf{T}_{\text{accum}} \leftarrow \{\}$.
- 4: **for** each text paragraph s_k^t in \mathbf{T} **do**
- 5: Add text paragraph s_k^t to accumulated text $\mathbf{T}_{\text{accum}} \leftarrow \mathbf{T}_{\text{accum}} \cup \{s_k^t\}$.
- 6: Initialize maximum confidence score $\text{max_score} \leftarrow 0$.
- 7: Initialize selected image $s_{\text{selected}}^i \leftarrow \text{None}$.
- 8: **for** each image s_j^i in candidate image set \mathbf{I}_c **do**
- 9: Provide image s_j^i and accumulated text $\mathbf{T}_{\text{accum}}$ to the LVLMS.
- 10: Compute confidence score c_j for image s_j^i .
- 11: **if** $c_j > \text{max_score}$ **then**
- 12: Update $\text{max_score} \leftarrow c_j$.
- 13: Update $s_{\text{selected}}^i \leftarrow s_j^i$.
- 14: **end if**
- 15: **end for**
- 16: Append selected image s_{selected}^i to order \mathbf{O}_p .
- 17: Remove selected image s_{selected}^i from candidate image set \mathbf{I}_c .
- 18: **end for**
- 19: **return** \mathbf{O}_p

predicted image insertion order \mathbf{O}_p . Assuming $\mathbf{O}_p = \{\text{None}, d_2^i, s_1^i, \text{None}, \text{None}, d_5^i\}$, by comparing \mathbf{O}_{gt} and \mathbf{O}_p , we calculate $\text{Acc}_i = 1/2 = 50\%$, $\text{Acc}_{ni} = 3/4 = 75\%$, $\text{Acc}_b = 4/7 = 57\%$.

Data Collection and Statistics

The primary challenge in collecting data for the FTII task lies in accurately determining the sequence of image insertion. For general image-text sources on media platforms such as Twitter and Weibo, the sequence of image insertion often lacks professionalism and may contain a substantial amount of misleading information. Consequently, we have shifted our research focus to the news domain. News websites, such as Xinhua and BBC News, typically feature a large number of interwoven text and image reports, and due to the authoritative nature of news reporting, the image insertion sequence in news can be regarded as a reliable standard.

To this end, we meticulously curated 318 high-quality Chinese news articles from Xinhua News and 307 high-quality English news articles from BBC, covering 10 domains: politics, economics and business, sports, technology, entertainment, health and lifestyle, culture and education, environment, society, and military. For the Chinese news, we assigned an average of 6.5 keywords per domain, with each keyword corresponding to an average of 4.97 articles. For the English news, we assigned an average of 6 keywords per

Paragraph 1 = “Just Stop Oil” issued a statement on social media platform Twitter, saying that at 8:30 a.m. local time on Monday, members of the organization sprayed orange paint from fire extinguishers onto the UK Home Office building, the MI5 building, the Bank of England, and the News Corp headquarters at London Bridge. The organization is attempting to pressure UK authorities to halt all new fossil fuel projects.



Paragraph 2 = **Paragraph 1** + “Just Stop Oil” is a radical environmental organization in the UK whose goal is to prevent the government from developing new oil and gas projects. The group has drawn attention for repeatedly targeting and damaging world-renowned artworks, including Van Gogh’s *Sunflowers* and *Peach Blossom*, Horatio McCulloch’s famous painting *My Heart’s in the Highlands*, and a wax figure of King Charles of the UK.



Paragraph 3 = **Paragraph 2** + When protesters were spraying paint on the exterior wall of MI5, a citizen quickly rushed to stop them. During the scuffle, the protester continued spraying paint. After seizing the paint can, the man with the backpack aimed the nozzle at the protester and sprayed them. Both individuals ended up covered in a large amount of paint.



Paragraph 4 = **Paragraph 3** + Finally, the man yanked off the protester’s hat and threw it aside, shouting loudly, which caused the protester to stop. On Twitter, the citizen who stopped the protester received widespread applause, with many netizens calling him a “hero.”



Paragraph 5 = **Paragraph 4** + Coincidentally, last Saturday, several protesters from the organization also clashed with London residents. On that day, the protesters occupied several major streets in the UK, obstructing traffic, and called on the government to immediately halt all fossil fuel projects. At that time, some frustrated drivers, having reached their limit, got out of their cars and physically removed the demonstrators.



⦿ Traverse the given set of images and select the most suitable one for insertion, providing its confidence level.

⦿ I think **B** is the most suitable, with a confidence level of **80%**. The groundtruth is **B**.

⦿ Traverse the given set of images and select the most suitable one for insertion, providing its confidence level.

⦿ I think **F** is the most suitable, with a confidence level of **70%**. The groundtruth is **G**.

⦿ Traverse the given set of images and select the most suitable one for insertion, providing its confidence level.

⦿ I think **E** is the most suitable, with a confidence level of **70%**. The groundtruth is **E**.

⦿ Traverse the given set of images and select the most suitable one for insertion, providing its confidence level.

⦿ I think **D** is the most suitable, with a confidence level of **85%**. The groundtruth is **‘no image’**.

⦿ Traverse the given set of images and select the most suitable one for insertion, providing its confidence level.

⦿ I think **‘no image’** is the most suitable, with a confidence level of **60%**. The groundtruth is **D**.

Figure 2: An example of a flow-insertion question in FTII-Bench. In a flow-insertion question, news text paragraphs are provided cumulatively, and the corresponding ground truth images are presented alongside other distracting images as options.

domain, with each keyword corresponding to an average of 5.12 articles. The statistical information of the data is shown in Figure 3.

FTII-Bench

Based on the collected image-text news data, we construct FTII-Bench, which includes two types of tasks: single-choice questions and flow-insertion questions. The single-choice questions are designed with four levels of difficulty, while the flow-insertion questions feature three different lev-

els of difficulty.

Single-choice question In our collected data, only a small portion of text paragraphs have the following image. Therefore, for the single-choice question, we use only those text paragraphs that are followed by images. Subsequently, in addition to the ground truth image, we introduce two additional images as distractors. By controlling the source of these distractor images, we adjust the difficulty levels of the single-choice question. Specifically, the questions are divided into

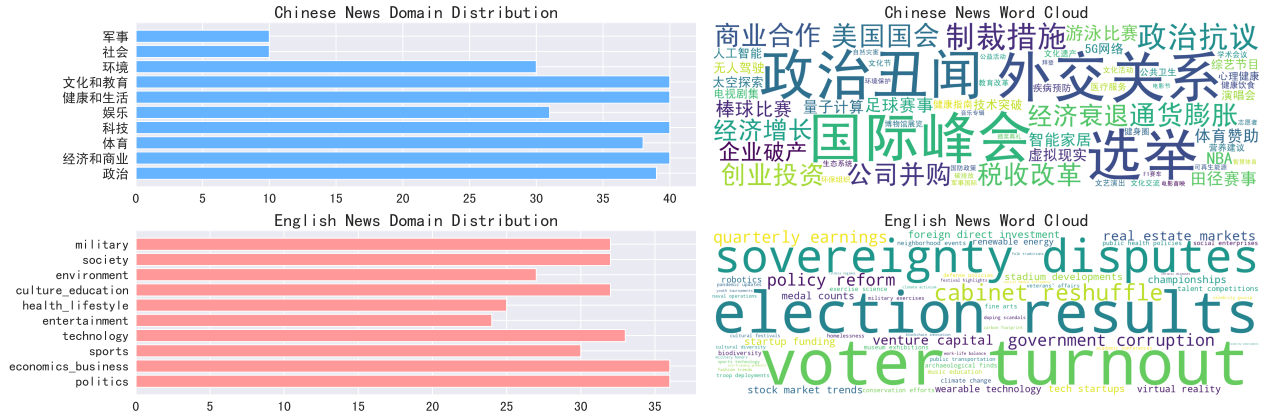


Figure 3: Data statistics regarding 318 high-quality Chinese news articles and 307 high-quality English news articles.

four difficulty levels, with Level 1 being the easiest and Level 4 the hardest.

- **Level 4 Difficulty:** Distractor images are sourced from the same news article. These images are usually highly similar, posing a significant challenge to the model’s judgment.
- **Level 3 Difficulty:** Distractor images come from the same domain and keyword but are from different news articles. This increases the similarity among images, though the contextual background varies between articles.
- **Level 2 Difficulty:** Distractor images are from the same domain but have different keywords and news articles. This makes the distractor images related in domain but different in topic and content.
- **Level 1 Difficulty:** Distractor images are from different domains, keywords, and news articles. In this setup, the distractor images have the least relevance to the question, offering the lowest difficulty.

By finely controlling the sources of distractor images, we can more effectively assess the model’s discriminative ability under different scenarios. As shown in Figure 1, this is an example of a single-choice question.

Flow-insertion question Unlike single-choice questions, Flow-insertion questions combine images from multiple news articles to form a set of candidate images, as represented by I_c in Algorithm 1. Similar to single-choice questions, Flow-insertion questions are divided into three difficulty levels based on the sources of the distractor images, with difficulty increasing from Level 1 to Level 3.

- **Level 3 Difficulty:** Distractor images come from the same domain and share the same keywords. This setup presents the greatest challenge due to the high similarity among the images.
- **Level 2 Difficulty:** Distractor images are sourced from the same domain but have different keywords. This variation introduces moderate difficulty by altering the context while maintaining domain relevance.

| Lan. | Level | # Questions | Avg. Word Count |
|------|-------|-------------|-----------------|
| CN | 4 | 409 | 141.34 |
| | 3 | 907 | 153.01 |
| | 2 | 907 | 158.01 |
| | 1 | 843 | 153.51 |
| EN | 4 | 711 | 35.60 |
| | 3 | 1079 | 25.73 |
| | 2 | 1084 | 35.14 |
| | 1 | 1032 | 35.83 |

Table 1: Statistical analysis for single-choice questions.

| Lan. | Level | # Questions | Avg. Word Count | Avg. # Images |
|------|-------|-------------|-----------------|---------------|
| CN | 3 | 318 | 1093.35 | 13.95 |
| | 2 | 590 | 1130.89 | 14.75 |
| | 1 | 749 | 1064.85 | 19.50 |
| EN | 3 | 307 | 621.84 | 18.07 |
| | 2 | 630 | 629.56 | 17.45 |
| | 1 | 665 | 609.23 | 24.13 |

Table 2: Statistical analysis for flow-insertion questions.

- **Level 1 Difficulty:** Distractor images originate from different domains and keywords. This provides the easiest level, as the distractor images have minimal relevance to the context of the question.

This hierarchical structuring of difficulty levels allows for a nuanced evaluation of the model’s ability to discern relevant images under varying conditions. As shown in Figure 2, this is an example of a Flow-insertion question.

Furthermore, we conducted statistical analysis on the different difficulty levels of Single-choice questions and Flow-insertion questions separately, as shown in Tables 1 and 2.

Experiments

In this section, we evaluate the performance of existing open-source and closed-source LVLMs, as well as CLIP-based models, on FTII-Bench. For single-choice questions,

| Model | Size | Level 1 | | Level 2 | | Level 3 | | Level 4 | |
|---------------------|------|---------|------|---------|------|---------|------|---------|------|
| | | EN | CN | EN | CN | EN | CN | EN | CN |
| Open-source LVLMS | | | | | | | | | |
| Llava-v1.5 | 7B | 34.6 | 33.7 | 33.5 | 32.5 | 33.5 | 32.0 | 31.6 | 33.0 |
| Llava-v1.5 | 13B | 33.9 | 32.4 | 34.2 | 32.5 | 32.3 | 31.5 | 32.8 | 34.7 |
| Idenfics2 | 8B | 31.9 | 31.8 | 33.1 | 34.7 | 32.7 | 31.1 | 35.4 | 34.7 |
| Fuyu | 8B | 32.7 | 9.3 | 33.2 | 11.2 | 33.1 | 9.3 | 33.2 | 6.8 |
| InstructBLIP | 11B | 35.3 | 21.8 | 33.5 | 21.1 | 31.6 | 21.5 | 33.1 | 20.0 |
| Kosmos2 | 1.6B | 35.4 | 18.0 | 32.9 | 16.9 | 33.8 | 17.2 | 33.2 | 22.5 |
| MiniCPM-V | 8B | 25.4 | 33.1 | 26.6 | 34.8 | 27.6 | 32.2 | 25.5 | 30.1 |
| Qwen-VL-Chat | 7B | 34.0 | 33.3 | 34.1 | 29.7 | 31.7 | 31.5 | 31.5 | 33.5 |
| XComposer2.5 | 7B | 50.2 | 47.6 | 49.6 | 47.2 | 44.4 | 37.8 | 37.8 | 34.2 |
| Closed-source LVLMS | | | | | | | | | |
| GPT-4o | - | 98.3 | 98.4 | 96.8 | 97.2 | 93.0 | 91.8 | 74.3 | 65.0 |
| GPT-4o-mini | - | 96.3 | 97.7 | 94.5 | 94.2 | 86.4 | 85.0 | 63.6 | 57.0 |
| CLIP-based models | | | | | | | | | |
| BGE-M3 | - | 90.6 | 92.1 | 85.0 | 85.0 | 78.1 | 67.6 | 55.0 | 45.7 |
| BGE-v1.5-en | - | 85.7 | - | 82.6 | - | 76.4 | - | 50.1 | - |

Table 3: The evaluation results of single choice questions in FTII-Bench: All questions are single-choice with three options, and accuracy (%) is used as the evaluation metric.

we input a text passage along with three image options into the LVLMS simultaneously. Due to the simultaneous input of multiple images, we follow the setup in (Jiang et al. 2024) and adopt two strategies to process these images: one strategy horizontally concatenates the images into a single image (‘merge’), while the other inputs the images sequentially into the model (‘sequence’). For the flow-insertion questions, we first provide a text paragraph and then sequentially traverse the image set, combining each image with the text paragraph as input to the LVLMS. It is important to emphasize that each input consists of only a single image. The detailed process is shown in Algorithm 1.

Baseline

Open-source LVLMS For the ‘merge’ validation method, we use Fuyu-8B (Bavishi et al. 2023), InstructBLIP-FlanT5-XXL (Dai et al. 2023), Kosmos2 (Peng et al. 2023), Llava-v1.5-7B (Liu et al. 2024a), Llava-v1.5-13B (Liu et al. 2024a), and Qwen-VL-Chat (Bai et al. 2023). For the ‘sequence’ validation method, we adopt Idenfics2 (Laurençon et al. 2024), MiniCPM-Llama3-V-2.5 (Yao et al. 2024), and XComposer2.5 (Zhang et al. 2024).

Close-source LVLMS We employ the latest GPT-4o and GPT-4o-mini models, and conduct evaluations based on a ‘sequence’ approach for single-choice questions.

CLIP-based model Compared to LVLMS, CLIP-based models lack the capability to follow instructions. Therefore, when handling single-choice questions, we first provide a text passage, which is encoded using a CLIP-based model to generate the corresponding text embedding. We then encode the three candidate images separately to generate their respective image embeddings and calculate the

cosine similarity between these and the text embedding, selecting the image with the highest score as the output. For flow-insertion questions, after obtaining the text embedding, the CLIP-based model traverses each image in the set, encodes it to generate its embedding, and calculates the cosine similarity with the text embedding, selecting the one with the highest score as the output. However, it is important to note that for flow-insertion questions, we introduce a threshold (set to 0.5 by default in this paper), and only when the highest score exceeds this threshold is the image considered as the output; otherwise, the output is recorded as ‘None.’ The CLIP-based models used in this paper include BGE-M3 (Chen et al. 2024) and BGE-v1.5-en (Xiao et al. 2023).

Single-choice Question Results

For single-choice questions, we set the task to select one out of three options: given a piece of text and three candidate images, the model is required to output the most suitable image to be inserted. Across different sub-datasets, the difficulty level gradually increases from 1 to 4 based on the source of the images.

Table 3 presents the evaluation results of CLIP-based models and LVLMS on FTII-Bench single-choice questions. It is observed that in CLIP-based models, the accuracy of the BGE model gradually decreases as the difficulty level increases, indicating that adjusting question difficulty by controlling the source of distractor images is an effective strategy. Among closed-source LVLMS, GPT-4o performs the best, achieving over 90% accuracy in the first three difficulty levels. However, at Level 4 Chinese difficulty, GPT-4o’s accuracy significantly drops to 65.0%, demonstrating that our benchmark poses a considerable challenge to existing LVLMS, presenting new difficulties.

Among open-source LVLMS, XComposer2.5-7B stands

| Model | EN | | | | | | | | | CN | | | | | | | | |
|----------------------------|------------------|------------------|-------------------|------------------|------------------|-------------------|------------------|------------------|-------------------|------------------|------------------|-------------------|------------------|------------------|-------------------|------------------|------------------|-------------------|
| | Level 1 | | | Level 2 | | | Level 3 | | | Level 1 | | | Level 2 | | | Level 3 | | |
| | Acc _b | Acc _i | Acc _{ni} | Acc _b | Acc _i | Acc _{ni} | Acc _b | Acc _i | Acc _{ni} | Acc _b | Acc _i | Acc _{ni} | Acc _b | Acc _i | Acc _{ni} | Acc _b | Acc _i | Acc _{ni} |
| <i>Open-source LVLMS</i> | | | | | | | | | | | | | | | | | | |
| Llava-v1.5-7B | 37.3 | 2.7 | 41.0 | 44.1 | 8.2 | 49.9 | 53.5 | 2.9 | 61.4 | 26.9 | 11.1 | 31.0 | 37.4 | 8.3 | 45.2 | 34.6 | 5.7 | 44.6 |
| Llava-v1.5-13B | 90.3 | 0 | 100.0 | 86.1 | 0 | 100.0 | 86.4 | 0 | 100.0 | 54.6 | 2.2 | 68.4 | 44.4 | 2.8 | 55.6 | 52.9 | 2.9 | 70.3 |
| Idenfics2 | 36.0 | 10.8 | 38.7 | 42.0 | 9.8 | 47.2 | 52.3 | 2.9 | 60.1 | 20.0 | 2.2 | 24.6 | 28.1 | 13.9 | 31.9 | 33.8 | 22.9 | 37.6 |
| Fuyu | 65.0 | 0 | 72.0 | 62.5 | 1.6 | 72.3 | 64.7 | 0 | 74.9 | 39.8 | 4.4 | 49.1 | 46.2 | 25.0 | 51.9 | 39.7 | 11.4 | 49.5 |
| InstructBLIP | 51.4 | 5.4 | 56.4 | 48.9 | 3.3 | 56.2 | 60.9 | 0 | 70.4 | 56.9 | 4.4 | 70.8 | 60.2 | 11.1 | 73.3 | 59.6 | 5.7 | 78.2 |
| Kosmos2 | 82.5 | 0 | 91.3 | 78.2 | 1.6 | 90.5 | 79.5 | 0 | 91.9 | 64.8 | 4.4 | 80.7 | 67.2 | 5.6 | 83.7 | 69.9 | 17.1 | 88.1 |
| MiniCPM-V | 35.8 | 0 | 39.6 | 41.4 | 3.3 | 47.5 | 51.9 | 0 | 60.1 | 22.2 | 8.9 | 25.7 | 34.8 | 29.2 | 19.4 | 31.9 | 11.4 | 38.6 |
| Qwen-VL-Chat | 57.2 | 8.1 | 62.4 | 50.1 | 3.3 | 58.6 | 59.3 | 2.9 | 68.2 | 35.2 | 4.4 | 43.4 | 30.4 | 16.7 | 34.1 | 35.3 | 20.0 | 40.6 |
| XComposer2.5 | 90.3 | 0 | 100.0 | 42.3 | 3.3 | 48.5 | 53.1 | 2.9 | 61.0 | 53.7 | 6.7 | 66.1 | 52.6 | 8.3 | 64.4 | 51.5 | 14.3 | 64.4 |
| <i>Closed-source LVLMS</i> | | | | | | | | | | | | | | | | | | |
| GPT-4o | 81.7 | 8.1 | 89.6 | 73.2 | 8.2 | 83.6 | 70.9 | 5.7 | 81.2 | 63.4 | 8.9 | 77.8 | 56.7 | 11.1 | 68.9 | 53.7 | 25.7 | 63.4 |
| GPT-4o-mini | 83.1 | 10.8 | 90.8 | 75.9 | 8.2 | 86.8 | 72.9 | 0 | 84.3 | 53.2 | 6.7 | 65.5 | 54.4 | 16.7 | 64.4 | 55.1 | 25.7 | 65.3 |
| <i>CLIP-based models</i> | | | | | | | | | | | | | | | | | | |
| BGE-M3 | 76.7 | 6.6 | 86.5 | 75.1 | 5.7 | 85.1 | 70.0 | 2.9 | 78.9 | 61.4 | 13.5 | 74.1 | 58.7 | 12.9 | 70.7 | 47.3 | 12.6 | 56.5 |
| BGE-v1.5-en | 65.9 | 6.0 | 74.3 | 64.6 | 5.7 | 73.1 | 60.8 | 1.9 | 68.6 | - | - | - | - | - | - | - | - | - |

Table 4: The evaluation results of flow-insertion questions in FTII-Bench.

out as the best-performing model. It achieves accuracy rates of 50.2% and 47.6% on Level 1 tasks in Chinese and English, respectively, significantly outperforming other models. Even on the relatively challenging Level 3 English tasks, it manages an accuracy of 44.4%. In contrast, other open-source LVLMS exhibit accuracy close to random guessing across four levels of difficulty. This poor performance in multi-image input scenarios is also observed in (Fu et al. 2024; Jiang et al. 2024). A possible reason for this underperformance is that these models were trained with limited or no use of multi-image input modes and related instructions, leading to suboptimal performance on multi-image tasks. Unlike others, XComposer2.5-7B employs the Unified Dynamic Image Partition strategy during training, which supports various input modes, including text, single-image, multi-image, and video inputs. This enables XComposer2.5-7B to excel in complex visual tasks, particularly outperforming other open-source LVLMS in multi-image scenarios.

Flow insert Question Results

In addressing the flow-insertion questions, we adopt an incremental approach to construct text paragraphs, while determining the most suitable image for insertion by traversing the candidate image set, as shown in Figure 2 and Algorithm 1. The evaluation results of the flow-insertion questions are presented in Tables 4. The results from both the English and Chinese tasks reveal a decline in accuracy across both BGE models as the task difficulty increases. For instance, in the English task, Acc_b of BGE-v1.5-en decreases from 65.9% at Level 1 to 64.6% at Level 2, and further to 60.8% at Level 3; similar trends are observed for other metrics. In the Chinese task, Acc_b of BGE-M3 drops from 61.4% at Level 1 to 58.7% at Level 2, and further to 47.3% at Level 3. This further validates the effectiveness of adjusting task difficulty by controlling the source of distractor images. Specifically, as

the difficulty increases, the similarity between groundtruth and distractor images grows, leading to a performance decline in CLIP-based models.

For LVLMS, the flow-insertion questions, unlike single-choice questions, not only tests the model’s image understanding capabilities but also challenges its comprehension of long texts and adherence to complex instructions. Current LVLMS generally perform poorly on this task. For instance, as shown in Table 4 EN, we observe that the Llava-v1.5-13B achieves an Acc_i of 0% across all three difficulty levels, while its Acc_{ni} is 100%. This indicates a significant deficiency in Llava-v1.5-13B’s understanding of whether an image should be inserted and its confidence level, leading to the model consistently selecting answers that do not require an image. Similar issues are observed in other models, such as Fuyu-8b, Kosmos2, and MiniCPM-V. These findings reveal the limitations of current LVLMS in understanding and following complex instructions. Furthermore, the extremely poor performance on the flow-insertion questions further underscores the limitations of current LVLMS when faced with multiple simultaneous challenges.

Conclusion

In this paper, we propose the Flow Text with Image Insertion task for the first time, introducing new challenges to existing LVLMS. We carefully compile a bilingual dataset of 625 entries, including 318 high-quality Chinese multimodal news items and 307 high-quality English multimodal news items. Based on these data, we introduce FTII-Bench, a benchmark comprising single-choice questions and highly challenging flow-insertion questions. The single-choice questions aim to assess the model’s multi-image understanding capability, while the flow-insertion questions comprehensively evaluate the model’s understanding of images, long texts, and complex instructions. Experimental results demonstrate that

even the most advanced closed-source LVLMS, such as GPT-4o, still face significant challenges in flow-insertion tasks. In the future, we plan to incorporate more data to fine-tune the models, further enhancing LVLMS’ performance when confronted with multiple competency evaluations.

References

- Alayrac, J.-B.; Donahue, J.; Luc, P.; Miech, A.; Barr, I.; Hasson, Y.; Lenc, K.; Mensch, A.; Millican, K.; Reynolds, M.; et al. 2022. Flamingo: a visual language model for few-shot learning. *Advances in neural information processing systems*, 35: 23716–23736.
- Anil, R.; Dai, A. M.; Firat, O.; Johnson, M.; Lepikhin, D.; Passos, A.; Shakeri, S.; Taropa, E.; Bailey, P.; Chen, Z.; et al. 2023. Palm 2 technical report. *arXiv preprint arXiv:2305.10403*.
- Bai, J.; Bai, S.; Yang, S.; Wang, S.; Tan, S.; Wang, P.; Lin, J.; Zhou, C.; and Zhou, J. 2023. Qwen-vl: A frontier large vision-language model with versatile abilities. *arXiv preprint arXiv:2308.12966*.
- Bavishi, R.; Elsen, E.; Hawthorne, C.; Nye, M.; Odena, A.; Somani, A.; and Taşlılar, S. 2023. Introducing our Multi-modal Models.
- Chen, J.; Xiao, S.; Zhang, P.; Luo, K.; Lian, D.; and Liu, Z. 2024. Bge m3-embedding: Multi-lingual, multi-functionality, multi-granularity text embeddings through self-knowledge distillation. *arXiv preprint arXiv:2402.03216*.
- Dai, W.; Li, J.; Li, D.; Tiong, A. M. H.; Zhao, J.; Wang, W.; Li, B. A.; Fung, P.; and Hoi, S. C. H. 2023. InstructBLIP: Towards General-purpose Vision-Language Models with Instruction Tuning. *ArXiv*, abs/2305.06500.
- Dosovitskiy, A.; Beyer, L.; Kolesnikov, A.; Weissenborn, D.; Zhai, X.; Unterthiner, T.; Dehghani, M.; Minderer, M.; Heigold, G.; Gelly, S.; et al. 2020. An image is worth 16x16 words: Transformers for image recognition at scale. *arXiv preprint arXiv:2010.11929*.
- Fu, X.; Hu, Y.; Li, B.; Feng, Y.; Wang, H.; Lin, X.; Roth, D.; Smith, N. A.; Ma, W.-C.; and Krishna, R. 2024. Blink: Multimodal large language models can see but not perceive. *arXiv preprint arXiv:2404.12390*.
- Gan, Z.; Li, L.; Li, C.; Wang, L.; Liu, Z.; Gao, J.; et al. 2022. Vision-language pre-training: Basics, recent advances, and future trends. *Foundations and Trends® in Computer Graphics and Vision*, 14(3–4): 163–352.
- Gao, J.; Ruan, J.; Xiang, S.; Yu, Z.; Ji, K.; Xie, M.; Liu, T.; and Fu, Y. 2024. LAMM: Label Alignment for Multi-Modal Prompt Learning. In *Proceedings of the AAAI Conference on Artificial Intelligence*, volume 38, 1815–1823.
- Jia, C.; Yang, Y.; Xia, Y.; Chen, Y.-T.; Parekh, Z.; Pham, H.; Le, Q.; Sung, Y.-H.; Li, Z.; and Duerig, T. 2021. Scaling up visual and vision-language representation learning with noisy text supervision. In *International conference on machine learning*, 4904–4916. PMLR.
- Jiang, D.; He, X.; Zeng, H.; Wei, C.; Ku, M.; Liu, Q.; and Chen, W. 2024. Mantis: Interleaved multi-image instruction tuning. *arXiv preprint arXiv:2405.01483*.
- Khattak, M. U.; Rasheed, H.; Maaz, M.; Khan, S.; and Khan, F. S. 2023. Maple: Multi-modal prompt learning. In *Proceedings of the IEEE/CVF Conference on Computer Vision and Pattern Recognition*, 19113–19122.
- Laurençon, H.; Tronchon, L.; Cord, M.; and Sanh, V. 2024. What matters when building vision-language models? *arXiv preprint arXiv:2405.02246*.
- Li, C.; Wong, C.; Zhang, S.; Usuyama, N.; Liu, H.; Yang, J.; Naumann, T.; Poon, H.; and Gao, J. 2024. Llava-med: Training a large language-and-vision assistant for biomedicine in one day. *Advances in Neural Information Processing Systems*, 36.
- Liu, H.; Li, C.; Li, Y.; and Lee, Y. J. 2024a. Improved baselines with visual instruction tuning. In *Proceedings of the IEEE/CVF Conference on Computer Vision and Pattern Recognition*, 26296–26306.
- Liu, H.; Li, C.; Wu, Q.; and Lee, Y. J. 2024b. Visual instruction tuning. *Advances in neural information processing systems*, 36.
- Liu, H.; Li, C.; Wu, Q.; and Lee, Y. J. 2024c. Visual instruction tuning. *Advances in neural information processing systems*, 36.
- Liu, Y.; Duan, H.; Zhang, Y.; Li, B.; Zhang, S.; Zhao, W.; Yuan, Y.; Wang, J.; He, C.; Liu, Z.; et al. 2023a. Mmbench: Is your multi-modal model an all-around player? *arXiv preprint arXiv:2307.06281*.
- Liu, Y.; Li, Z.; Yang, B.; Li, C.; Yin, X.; Liu, C.-l.; Jin, L.; and Bai, X. 2023b. On the hidden mystery of ocr in large multimodal models. *arXiv preprint arXiv:2305.07895*.
- Lu, P.; Bansal, H.; Xia, T.; Liu, J.; Li, C.; Hajishirzi, H.; Cheng, H.; Chang, K.-W.; Galley, M.; and Gao, J. 2023. Mathvista: Evaluating mathematical reasoning of foundation models in visual contexts. *arXiv preprint arXiv:2310.02255*.
- Masry, A.; Long, D. X.; Tan, J. Q.; Joty, S.; and Hoque, E. 2022. Chartqa: A benchmark for question answering about charts with visual and logical reasoning. *arXiv preprint arXiv:2203.10244*.
- Mathew, M.; Karatzas, D.; and Jawahar, C. 2021. Docvqa: A dataset for vqa on document images. In *Proceedings of the IEEE/CVF winter conference on applications of computer vision*, 2200–2209.
- OpenAI, R. 2023. Gpt-4 technical report. *arxiv* 2303.08774. *View in Article*, 2(5).
- Peng, Z.; Wang, W.; Dong, L.; Hao, Y.; Huang, S.; Ma, S.; and Wei, F. 2023. Kosmos-2: Grounding multimodal large language models to the world. *arXiv preprint arXiv:2306.14824*.
- Radford, A.; Kim, J. W.; Hallacy, C.; Ramesh, A.; Goh, G.; Agarwal, S.; Sastry, G.; Askell, A.; Mishkin, P.; Clark, J.; et al. 2021. Learning transferable visual models from natural language supervision. In *International conference on machine learning*, 8748–8763. PMLR.
- Rasheed, H.; khattak, M. U.; Maaz, M.; Khan, S.; and Khan, F. S. 2023. Finetuned CLIP models are efficient video learners. In *The IEEE/CVF Conference on Computer Vision and Pattern Recognition*.

- Ruan, J.; Gao, J.; Xie, M.; Dong, D.; Xiang, S.; Liu, T.; and Fu, Y. 2024a. iDAT: inverse Distillation Adapter-Tuning. In *2024 IEEE International Conference on Multimedia and Expo (ICME)*, 1–6. IEEE.
- Ruan, J.; Gao, J.; Xie, M.; Xiang, S.; Yu, Z.; Liu, T.; and Fu, Y. 2023. GIST: Improving Parameter Efficient Fine Tuning via Knowledge Interaction. *arXiv preprint arXiv:2312.07255*.
- Ruan, J.; Yuan, W.; Lin, Z.; Liao, N.; Li, Z.; Xiong, F.; Liu, T.; and Fu, Y. 2024b. MM-CamObj: A Comprehensive Multimodal Dataset for Camouflaged Object Scenarios. *arXiv preprint arXiv:2409.16084*.
- Singhal, K.; Tu, T.; Gottweis, J.; Sayres, R.; Wulczyn, E.; Hou, L.; Clark, K.; Pfohl, S.; Cole-Lewis, H.; Neal, D.; et al. 2023. Towards expert-level medical question answering with large language models. *arXiv preprint arXiv:2305.09617*.
- Touvron, H.; Lavril, T.; Izacard, G.; Martinet, X.; Lachaux, M.-A.; Lacroix, T.; Rozière, B.; Goyal, N.; Hambro, E.; Azhar, F.; et al. 2023. Llama: Open and efficient foundation language models. *arXiv preprint arXiv:2302.13971*.
- Wang, W.; Lv, Q.; Yu, W.; Hong, W.; Qi, J.; Wang, Y.; Ji, J.; Yang, Z.; Zhao, L.; Song, X.; et al. 2023a. Cogvlm: Visual expert for pretrained language models. *arXiv preprint arXiv:2311.03079*.
- Wang, W.; Xie, J.; Hu, C.; Zou, H.; Fan, J.; Tong, W.; Wen, Y.; Wu, S.; Deng, H.; Li, Z.; et al. 2023b. Drivemlm: Aligning multi-modal large language models with behavioral planning states for autonomous driving. *arXiv preprint arXiv:2312.09245*.
- Xiao, S.; Liu, Z.; Zhang, P.; and Muennighof, N. 2023. C-pack: Packaged resources to advance general chinese embedding. *arXiv preprint arXiv:2309.07597*.
- Xu, Z.; Zhang, Y.; Xie, E.; Zhao, Z.; Guo, Y.; Wong, K.-Y. K.; Li, Z.; and Zhao, H. 2024. Drivegpt4: Interpretable end-to-end autonomous driving via large language model. *IEEE Robotics and Automation Letters*.
- Yang, Z.; Lu, Y.; Wang, J.; Yin, X.; Florencio, D.; Wang, L.; Zhang, C.; Zhang, L.; and Luo, J. 2021. Tap: Text-aware pre-training for text-vqa and text-caption. In *Proceedings of the IEEE/CVF conference on computer vision and pattern recognition*, 8751–8761.
- Yao, Y.; Yu, T.; Zhang, A.; Wang, C.; Cui, J.; Zhu, H.; Cai, T.; Li, H.; Zhao, W.; He, Z.; et al. 2024. MiniCPM-V: A GPT-4V Level MLLM on Your Phone. *arXiv preprint arXiv:2408.01800*.
- Yuan, L.; Chen, D.; Chen, Y.-L.; Codella, N.; Dai, X.; Gao, J.; Hu, H.; Huang, X.; Li, B.; Li, C.; et al. 2021. Florence: A new foundation model for computer vision. *arXiv preprint arXiv:2111.11432*.
- Zhang, P.; Dong, X.; Zang, Y.; Cao, Y.; Qian, R.; Chen, L.; Guo, Q.; Duan, H.; Wang, B.; Ouyang, L.; Zhang, S.; Zhang, W.; Li, Y.; Gao, Y.; Sun, P.; Zhang, X.; Li, W.; Li, J.; Wang, W.; Yan, H.; He, C.; Zhang, X.; Chen, K.; Dai, J.; Qiao, Y.; Lin, D.; and Wang, J. 2024. InternLM-XComposer-2.5: A Versatile Large Vision Language Model Supporting Long-Contextual Input and Output. *arXiv preprint arXiv:2407.03320*.
- Zheng, L.; Chiang, W.-L.; Sheng, Y.; Zhuang, S.; Wu, Z.; Zhuang, Y.; Lin, Z.; Li, Z.; Li, D.; Xing, E.; et al. 2024. Judging llm-as-a-judge with mt-bench and chatbot arena. *Advances in Neural Information Processing Systems*, 36.
- Zhou, K.; Yang, J.; Loy, C. C.; and Liu, Z. 2022. Learning to prompt for vision-language models. *International Journal of Computer Vision*, 130(9): 2337–2348.
- Zhu, T.; Qu, X.; Dong, D.; Ruan, J.; Tong, J.; He, C.; and Cheng, Y. 2024. Llama-moe: Building mixture-of-experts from llama with continual pre-training. *arXiv preprint arXiv:2406.16554*.